

# Mathematical Modeling of Drip Emitter Discharge of Trapezoidal Labyrinth Channel

N. Philipova

**Abstract**—The influence of the geometric parameters of trapezoidal labyrinth channel on the emitter discharge is investigated in this work. The impact of the dentate angle, the dentate spacing, and the dentate height are studied among the geometric parameters of the labyrinth channel. Numerical simulations of the water flow movement are performed according to central cubic composite design using Commercial codes GAMBIT and FLUENT. Inlet pressure of the dripper is set up to be 1 bar. The objective of this paper is to derive a mathematical model of the emitter discharge depending on the dentate angle, the dentate spacing, the dentate height of the labyrinth channel. As a result, the obtained mathematical model is a second-order polynomial reporting 2-way interactions among the geometric parameters. The dentate spacing has the most important and positive influence on the emitter discharge, followed by the simultaneous impact of the dentate spacing and the dentate height. The dentate angle in the observed interval has no significant effect on the emitter discharge. The obtained model can be used as a basis for a future emitter design.

**Keywords**—Drip irrigation, labyrinth channel hydrodynamics, numerical simulations, Reynolds stress model.

## I. INTRODUCTION

INTERGOVERNMENTAL Panel on Climate Change (IPCC) at its fortieth meeting in Denmark (2014) has analyzed environmental impact of the climate changes. The combined land and ocean surface temperature data are globally averaged and calculated by a linear trend. This trend shows warming of 0.85 °C over the period 1880 to 2012. The rate of warming over the past 15 years (1998-2012) is 0.05 °C per decade. Over the period 1901-2010 global mean sea level rose by 0.19 m. It is very likely that the mean rate of global averaged sea level rise was 1.7 mm/year between 1901 and 2010 and 3.2 mm/year between 1993 and 2010. Extreme weather events including heat waves, heavy precipitations and coastal flooding are expecting to cause negative impact on average crop yields and increase in yield vulnerability due to the climate change [1].

Sustainable agriculture is one of the responses of the governmental policy not only for the European members, but it is valid for all the countries in the entire world. According to that, measures should be undertaken for developing smart technologies such as applying drip irrigation technology in order the mankind to succeed to combat with increasing food demands under conditions of insufficient water resources.

The drip emitter is a precise irrigation device for applying

small amounts of water by dissipating pressure energy along the labyrinth channel length. In-line emitters maintain turbulent flow that helps preventing clogging.

Several possible approaches are observed in investigating drippers' hydraulic behavior occurring in the last decades. The first one is to use Computational Fluid Dynamics (CFD) Commercial codes and Reynolds stress model (RSM) in particular, to simulate the water flow movement in the emitter labyrinth channel. On the basis of such simulations, the emitters' hydraulic performance is examined by [2], [3]. In addition, the emitter susceptibility to clogging is investigated by [4], [5]. Such numerical simulations help saving efforts and funds in the drip emitters' design and the testing.

A mathematical model of the emitter discharge of triangular, rectangular and trapezoidal labyrinth channels based on numerical simulations has been developed by [6]-[8]. A disadvantage of the last model is that it is performed with coded factors.

Another approach is to produce moulds for a real manufacture of the drip emitters. The number of the produced moulds and correspondingly drippers are determined by statistical methods. A relationship between the emitter discharge and four independent geometric parameters has been derived considering trapezoidal emitter labyrinth after the drippers' production and their embedding in the drip irrigation tapes [9].

Rapid Prototyping (RP) is a new technology which core idea is based on the dimension reduction discrete methods. A complex three-dimensional object (CAD file) is firstly sliced (STL files), and then converted into two-dimensional planes. The RP machine builds the object layer by layer and finally fabricating the part. Experimental tests were undertaken in the laboratory environment to verify and compare with the CFD results [10], [11].

The objective of this paper is to derive a mathematical model of the emitter discharge depending on the basic geometric parameters of labyrinth channel: the dentate spacing, the dentate height and the dentate angle. The objective of this work could be accomplished by performing numerical simulations of the water flow movement by using CFD Commercial codes. The inlet pressure of the emitter is set up at 1 bar.

## II. MATERIALS AND METHODS

### A. Model Equations

The flow regime is proved by experiments and simulations to be turbulent, although the Reynolds number is about 800 - much lower than 2300. Turbulent models such as standard

N. Philipova is with the Fluid Mechanics Department, Institute of Mechanics- Bulgarian Academy of Science, Sofia 1113, Bulgaria (e-mail: philipova@imbm.bas.bg).

$k-\varepsilon$ , RNG  $k-\varepsilon$ , Realizable  $k-\varepsilon$  can be used, but most of them only calculate the turbulent stress with isotropic turbulent viscosity and the rotary flow and variation of the surface curvature are not taken into account [12]. RSM is applied which can account for the effects of streamline curvature, swirl, rotation [3]-[5]. The flow is considered to be a viscous, steady, and incompressible. The model includes correspondingly the continuity equation and the Reynolds Averaged Navier-Stokes Equations [13]-[15]:

$$\frac{\partial}{\partial x_i}(\rho u_i) = 0 \quad (1)$$

$$\frac{\partial}{\partial x_i}(\rho u_i u_j) = -\frac{\partial p}{\partial x_j} + \frac{\partial}{\partial x_i} \left( \mu \frac{\partial u_i}{\partial x_j} - \rho \overline{u'_i u'_j} \right), \quad (i, j = 1, 2, 3) \quad (2)$$

where:  $u_i$  - the vector velocity,  $\rho$  - the water density,  $\mu$  - the fluid molecular viscosity, and  $\overline{u'_i u'_j}$  - the Reynolds stress tensor.

In (3), the left hand side term is the convection. The first term on the right hand side is the stress production term. The second term is the pressure-strain term. The third term is the sum of turbulent and molecular diffusion and the last term is the dissipation term:

$$\begin{aligned} \frac{\partial}{\partial x_i}(\rho u_k \overline{u'_i u'_j}) &= P_{ij} + \Phi_{ij} \\ &+ \frac{\partial}{\partial x_k} \left( \frac{\mu_t}{\sigma_k} \frac{\partial \overline{u'_i u'_j}}{\partial x_k} + \mu \frac{\partial \overline{u'_i u'_j}}{\partial x_k} \right) - \frac{2}{3} \rho \varepsilon \delta_{ij} \end{aligned} \quad (3)$$

The stress production term  $P_{ij}$  is given by (4):

$$P_{ij} = -\rho \left( \overline{u'_i u'_k} \frac{\partial u_j}{\partial x_k} + \overline{u'_j u'_k} \frac{\partial u_i}{\partial x_k} \right). \quad (4)$$

The pressure - strain term  $\Phi_{ij}$  is decomposed into two components which are the following:

$$\Phi_{ij,1} = -C_1 \rho \frac{\varepsilon}{k} \left( \overline{u'_i u'_j} - \frac{2}{3} k \delta_{ij} \right), \quad (5)$$

$$\Phi_{ij,2} = -C_2 \left( P_{ij} - \frac{2}{3} P_k \delta_{ij} \right), \quad (6)$$

where  $C_1 = 1.8$ ,  $C_2 = 0.6$  and  $\mu_t$  is the turbulent viscosity, linked to the turbulent kinetic energy  $k$  and the dissipation rate  $\varepsilon$  via the relation:

$$\mu_t = \rho C_\mu \frac{k^2}{\varepsilon} \quad (7)$$

The differential transport equations for  $k$  and  $\varepsilon$  are:

$$\frac{\partial(\rho k u_i)}{\partial x_i} = \frac{\partial}{\partial x_j} \left[ \left( \mu + \frac{\mu_t}{\sigma_k} \right) \frac{\partial k}{\partial x_j} \right] + \frac{1}{2} P_{ij} - \rho \varepsilon, \quad (8)$$

$$\frac{\partial(\rho \varepsilon u_i)}{\partial x_i} = \frac{\partial}{\partial x_j} \left[ \left( \mu + \frac{\mu_t}{\sigma_\varepsilon} \right) \frac{\partial \varepsilon}{\partial x_j} \right] + \frac{1}{2} C_{1\varepsilon} P_{ij} - C_{2\varepsilon} \rho \frac{\varepsilon^2}{k}, \quad (9)$$

where the model constants are the following:

$$\begin{aligned} C_\mu &= 0.09, \quad C_{1\varepsilon} = 1.44, \quad C_{2\varepsilon} = 1.92, \quad \sigma_k = 1, \\ \sigma_\varepsilon &= 1.3 \end{aligned} \quad (10)$$

Boundary conditions at the inlet face are  $x = x_{inlet}$ ,  $P_{inlet} = P_0$ . Initial conditions:  $t = 0$ ,  $P_{inlet} = P_0$ ,  $v_{inlet} = v_0$ .

Turbulent intensity is set up 15% and labyrinth channel hydraulic diameter is used as well to define the turbulence parameters of water flow movement along the labyrinth channel length.

Boundary conditions for Reynolds stresses are:

$$\frac{\overline{u'^2_\tau}}{u_\tau^2} = 5.1, \quad \frac{\overline{u'^2_\eta}}{u_\tau^2} = 1.0, \quad \frac{\overline{u'^2_\lambda}}{u_\tau^2} = 2.3, \quad -\frac{\overline{u'_\tau u'_\eta}}{u_\tau^2} = 1.0, \quad (11)$$

where:  $\tau$  - the tangential co-ordinate,  $\eta$  - the normal co-ordinate,  $\lambda$  - the bi-normal co-ordinate,  $u_\tau$  - the friction velocity [16].

The fluid velocity is constrained to be zero (non-slip conditions), and the standard log-law wall function is used to bridge the near-wall linear sublayer [4].

### B. Numerical Simulations

The water flow in the labyrinth channel is considered stationary and viscous and it is simulated by using the CFD Commercial codes GAMBIT and FLUENT. The geometry and the mesh of the labyrinth volume are created in GAMBIT. The labyrinth volume was meshed with hexahedral grid. The model equations and the boundary and the initial conditions are determined in FLUENT [16]. The aforementioned governing equations are discretized by the control volume technique, and then the SIMPLE pressure-velocity coupling technique is used.

### III. RESULTS AND DISCUSSION

The design of experiments is developed according to cubic central composite design with 14 planned experiments with the varying three factors on three levels (Table I). The observed parameters are the dentate angle  $\theta$ , the dentate spacing  $B$ , and the dentate height  $H$  (Fig. 1). The intervals of varying the observed geometric parameters are:  $\theta = 28^\circ \div 36^\circ$ ,  $B = 2 \div 2.5 \text{ mm}$ ,  $H = 1.0 \div 1.6 \text{ mm}$ .

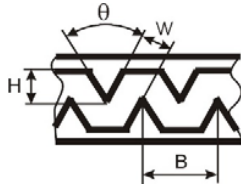


Fig. 1 Geometric parameters of the labyrinth channel:  $\theta$  - the dentate angle,  $H$  - the dentate height,  $B$  - the dentate spacing,  $W$  - the channel width

The dependent variable is the emitter discharge at the emitter outlet obtained as an output variable from the performed numerical simulations. The model equation (12) is a second-order polynomial reporting 2-way interactions among the observed parameters. The equation is derived by applying multiple regression of the Commercial code Statistika [17]. The obtained model equation has the following type:

$$q^{\text{mod}} = b_0 + b_1 B + b_2 BH \quad (12)$$

where:  $q^{\text{mod}}$  - the model emitter discharge,  $b_i$  - the coefficients.

Taking into account the coefficients  $b_i$  from Table II, the mathematical model of the emitter discharge of trapezoidal labyrinth channel is defined as it follows:

$$q^{\text{mod}} = -2.7988 + 3.52766 B - 0.537 BH \quad (13)$$

This equation has derived at inlet pressure at labyrinth channel equal to 1 bar. The data for the emitter discharge obtained by the numerical simulations are called  $q^{\text{exp}}$ . The mean absolute error is calculated according to the formula:

$$\delta = \left| q^{\text{exp}} - q^{\text{mod}} \right| / q_{\text{max}}, \quad (14)$$

where  $q_{\text{max}}$  is the maximum value between  $q^{\text{mod}}$  and  $q^{\text{exp}}$ .

The mean absolute error  $\delta$  between the experimental data  $q^{\text{exp}}$  and the model data  $q^{\text{mod}}$  for the examined trapezoidal labyrinth channel is 1.91%.

The dentate spacing  $B$  has the only main effect exerted on the emitter discharge. This effect is positive, i.e. the dentate spacing increasing leads to the emitter discharge increasing. The strongest impact and the only significant factors among the simultaneous influencing possess the dentate spacing  $B$  and the dentate height  $H$ . They have a negative effect on the emitter discharge. The strongest influence is observed at  $B = B_{\text{max}} = 2.5 \text{ mm}$  and  $H = H_{\text{min}} = 1.0 \text{ mm}$  ( $B_{\text{max}}$  is the maximum examined value of  $B$ ,  $H_{\text{min}}$  is the minimum examined value of  $H$ ). Emitter discharge data for experiments 3 and 4 are  $q = q_{\text{max}} = 4.68 \text{ l/h}$  for the aforementioned values of  $B$  and  $H$ . The model statistics indicates that the dentate angle  $\theta$  has no significant effect on the emitter discharge,

neither as a main effect, nor as a simultaneous effect with the other factors. The coefficients are significant when the p-value of the corresponding coefficients is lower than 0.05.

TABLE I  
CUBIC CENTRAL COMPOSITE DESIGN FOR THE EMITTER DISCHARGE MODEL DERIVING

No	$\theta$		$B$	$H$	$q^{\text{exp}}$	$q^{\text{mod}}$	$\delta$
	(deg)	(rad)	(mm)	(mm)	[l/h]	[l/h]	%
1	28°	0.489	2	1.0	3.2316	3.1825	1.29
2	36°	0.628	2	1.0	3.2439	3.1825	2.08
3	28°	0.489	2.5	1.0	4.6713	4.6779	0.023
4	36°	0.628	2.5	1.0	4.6778	4.6779	0.2
5	28°	0.489	2	1.6	2.5956	2.5381	0.88
6	36°	0.628	2	1.6	2.6413	2.5381	3.86
7	28°	0.489	2.5	1.6	3.8995	3.8724	0.38
8	36°	0.628	2.5	1.6	3.9128	3.8724	1.22
9	36°	0.628	2.25	1.3	3.3806	3.5677	4.42
10	28°	0.489	2.25	1.3	3.6808	3.5677	3.05
11	32°	0.559	2.5	1.3	4.2401	4.2751	1.04
12	32°	0.559	2	1.3	2.6985	2.8603	7.35
13	32°	0.559	2.25	1.6	3.084	3.2052	0.55
14	32°	0.559	2.25	1.0	3.9147	3.9302	0.44

1.91%

TABLE II  
STATISTICS OF THE EMITTER DISCHARGE MODEL

	Estimate	Standard error	t-value df = 11	p-level	Lo. Conf Limit	Up. Conf Limit
b <sub>0</sub>	-2.79881	0.277995	-10.0679	0.000001	-3.41068	-2.18695
b <sub>1</sub>	3.52766	0.136403	25.8621	0.000000	3.22744	3.82788
b <sub>2</sub>	-0.53697	0.045337	-11.8440	0.000000	-0.63675	-0.43718

The value of multiple correlation coefficient squared is  $R^2 = 0.9838$ , and  $R = 0.99188$ , that proves an excellent agreement between the experimental and the model data of the trapezoidal labyrinth channel.

#### IV. CONCLUSIONS

In this paper, a mathematical model of the emitter discharge is derived depending on the geometric parameters of trapezoidal labyrinth channel. It is based on the multiple regression of 14 planned numerical experiments including the varying of three factors on three levels. The following conclusions can be drawn taking into account the derived model:

- 1) The dentate spacing  $B$  has the only main and positive effect exerted on the emitter discharge.
- 2) The dentate spacing  $B$  and the dentate height  $H$  have the simultaneous influence on the emitter discharge
- 3) The coefficients of the model are statistically significant ( $p < 0.05$ ). The value of multiple correlation coefficient squared is  $R^2 = 0.9838$ , and  $R = 0.99188$ , that shows an excellent agreement between the experimental and the model data.

Both obtained models of the emitter discharge and pressure losses can be used as a basis for an optimization for the determining the optimum values of the geometric parameters

of the drip emitter labyrinth channel. That will be an important step in a more successful “in-line” drip emitter design.

## REFERENCES

- [1] Intergovernmental Panel on Climate Change. Synthesis Report, 2014, Denmark Available at: [http://www.ipcc.ch/pdf/assessment-report/ar5/syr/SYR\\_AR5\\_FINAL\\_full\\_wcover.pdf](http://www.ipcc.ch/pdf/assessment-report/ar5/syr/SYR_AR5_FINAL_full_wcover.pdf).
- [2] Y. Li, P. Yang, S. Ren, “Hydraulic characterization of tortuous flow in path drip irrigation emitter”, *J. of Hydrodynamics, Ser. B*, vol. 18, no 4, 2006, pp. 449-457.
- [3] J. Zhang, W. Zhao, Y. Tang, Z. Wei, B. Lu, “Numerical investigations of the clogging mechanism in labyrinth channel of the emitter”, *Int. J. for Num. Meth. in Eng.*, vol. 70, 2007, pp.1598-1612.
- [4] J. Zhang, W. Zhao, Z. Wei, Y. Tang, B. Lu, “Numerical and experimental study on hydraulic performance of emitters with arc labyrinth channel”, *Computers and Electronics in Agriculture*, vol. 56, 2007, pp.120-129.
- [5] D. Yan, P. Yang, S. Ren, Y. Li, “Numerical study on flow property in dentate path of drip emitters”, *New Zealand J. of Agr. Research*, vol. 50, 2007, pp. 705-712.
- [6] N. Philipova, N. Nikolov, G. Pichurov, D. Markov, “A mathematical model of emitter discharge depending on geometric parameters of drip emitter labyrinth channel” ,*Proc of the 11<sup>th</sup> National Congress on Theoretical and Applied Mechanics*, 2-5 Sept. 2009, Borovets, Bulgaria (CD-ROM), pp. 1-6.
- [7] N. Philipova, N. Nikolov, E. Stoimenova, G. Pichurov, D. Markov, “Mathematical Modeling Drip Emitter Discharge of Triangle Labyrinth Channel”, *Comptesrendusdel’Academiebulgare des Scinces*, vol. 64, no 1, 2011. Pp.133-140.
- [8] N. Philipova, N. Nikolov, E. Stoimenova, G. Pichurov, D. Markov, “A regression equation of drip emitter discharge depending on the geometric parameters of rectangular labyrinth channel”, *Comptesrendusdel’Academiebulgare des Scinces*, vol. 64, no 11, 2011, pp. 1607-1614.
- [9] G. Li, J. Wang, M. Alam, Y. Zhao, “Influence on geometric parameters of labyrinth flow path of drip emitters on hydraulic and anti-clogging performance”, *Transactions of ASABE*, vol.49, no 3, 2006, pp. 637- 643.
- [10] Mohammed Ali, “Anticlogging Drip Irrigation Emitters Design Innovation”, *European International Journal of Science and Technology*, vol.2, no 8, 2013, pp. 154-164.
- [11] Z. Wei, “Application of RP and Manufacturing to water-saving emitters”, in *Advanced Application of Rapid Prototyping Technology in Modern Engineering*, Available at: <http://www.intechopen.com/books/advanced-applications-of-rapid-prototyping-technology-in-modern-engineering/application-of-rp-and-manufacturing-to-water-saving-emitter>.
- [12] Zhao, W., Zhang, J, Tang, Y., Wei, Z., Lu, B., IFIO International Federation for Information Processing, Vol.294, Computer and Computing Technologies in Agriculture II, vol. 2, 2009, eds D. Li, Z. Chunjiang, Boston: Springer, pp.881-890
- [13] K. Hanjalic, B. Launder, “A Reynolds stress model of turbulence and its application to thin shear flows”, *J. Fluid Mech.*, vol.52, no 4, 1972, pp. 609-638.
- [14] B. Launder, G. Reece, W. Rodi, “Progress in the development of a Reynolds- stress turbulence closure”, *J. Fluid Mech.*, vol. 68, no 3, 1975, pp. 537-566.
- [15] H. Versteeg, W. Malalasekera, *An Introduction to Computational Fluid Dynamics: The Finite Volume Method*, Willey, New York, 1995.
- [16] Fluent 6.3 User’s Guide, Available at: [https://www.sharcnet.ca/Software/Fluent6/html/ug/main\\_pre.htm](https://www.sharcnet.ca/Software/Fluent6/html/ug/main_pre.htm).
- [17] StatSoft Electronic Statistics Textbook, 2010, Available at <http://www.statsoft.com/textbook>.